Chapter

HYSTERESIS MODULATION IN STRUCTURAL CONTROL SYSTEMS AND SEMI-ACTIVE IMPLEMENTATION

Marco Domaneschi[*]

Politecnico di Milano, Department of Civil and
Environmental Engineering, Milan, Italy

ABSTRACT

Models of hysteresis are employed for simulating control devices in complex structural systems. This chapter is devoted firstly to review the existent literature on passive control system modeling. Subsequently, the exposition is focused on their innovative development represented by the semi-active improvement as one of the most recent solutions in the field of numerical simulation of structural control systems. Some examples of application are finally given.

Keywords: Structural Control, Passive, Semi-active, Numerical Simulation

INTRODUCTION

Phenomenological models of mechanical passive systems with hysteresis can be employed for simulating dampers or isolation devices into structural models, both with the aim of evaluating their effects at a design stage for new buildings or for a supplementary implementation on existing ones. Their mathematical formulation usually allows their application in refined structural finite element models or in simpler closed form analytical approaches.

---

[*] Corresponding author: Marco Domaneschi. Piazza Leonardo da Vinci 32, 20133, Milan Italy. E-mail: marco. domaneschi@polimi.it.

A review of existing literature in the field of passive systems modeling is summarized in the first section of the chapter, spreading from recent advances on the dissipative models of hysteresis to numerical solution adopted for reproducing the characteristics of base-isolation systems, with special care to rubber bearings.

An innovative semi-active technology for control systems has been introduced in recent decades as a progress toward more efficient and adaptable solutions, with respect to the classical passive ones. Several examples are reported to the aim of describing the current research trend. Rearranging control reactions simultaneously with the hazardous excitation, provides enhanced structural behavior for improved usefulness and safety. Consequently, current numerical simulation procedures, which proved to be effective for the passive implementation, are expected to include the semi-active description as well.

Along with, the second section of the chapter is focused on existent numerical methodologies for simulating the semi-active modulation of hysteresis components in real time. A recently proposed semi-active developments of a wide employed passive model is discussed. Special attention will be given to the use of the innovative model for design issues and to its adoption in developing new semi-active control laws for driving semi-active dissipative devices. The theoretical formulation of the original settlement is discussed, allowing to focus on the way for tuning the parameters which can be modified on-line for modulating the dissipative component. Therefore, special care is given to the methodology for embedding new algorithms into the analytical formulation of the model and for testing their efficiency.

In the remaining of this chapter, the general capability of the previously discussed numerical approaches is presented with applications to complex structural systems and reference to existing studies from literature. Mitigation of direct dynamic effects (e.g. acceleration, displacements) induced by earthquake and wind loadings represents the most expected purpose of structural control discipline.

However, in conclusion, attention is also given to the positive outcomes related to indirect effects, coming from the dampers implementation on buildings.

OVERVIEW ON STRUCTURAL CONTROL

Passive systems of vibration protection can be presented as the simplest typology of structural control solutions: the control device works without using data collected from other elements as sensors. The passive protection can be considered asymptotically stable.

Active systems are the most effective in the vibration protection of mechanical systems. However, they are complicated by a large number of elements which participate in the input data processing and the formation of the control forces. They are sensors, actuator devices, and other facilities, acting in the amplification and manipulation of data.

The *Semi-active* system can be considered as passive system with smart qualities: they able to change actively its characteristic, driven by an external command, manually or automatically.

Hybrid control systems employ at the same time passive solutions with active or semi-active ones. When active or semi-active systems are considered, the control forces are processed by special algorithms collecting informations on the current conditions from an open or a closed loop data flow.

An open loop control system is a combination in series of elements, from a starting point to another point in a flow scheme. Its transfer function is the result of the product of each single element transfer function. A closed-loop system is a combination of elements with feedback connection [1].

PASSIVE NUMERICAL MODELS OF HYSTERESIS

The Bouc-Wen Model

The most eclectic phenomenological model of hysteretic mechanical systems reported in the present literature is probably the Bouc-Wen (BW) endochronic model [2, 3]. It has been selected by several Authors for the simulation of the hysteretic component for a wide range of control devices. The physical and mathematical consistency of that model [4] and the excellent correspondence between the experimental and numerical results are probably the main reasons which support and justify its frequent implementation. In this section the general approach to the oscillator dynamic equation with the BW model is summarized [5] and a number of results reported in the literature are also summarized.

A hysteretic oscillator can be represented by the following equation of motion [6]:

$$m\ddot{x} + c\dot{x} + \Phi(x, \dot{x}) = f(t) \tag{1}$$

where x is the displacement, the simple superimposed dot means the first time derivative (velocity) and the double superimposed dot the second time derivative (acceleration). In equation (1), $f(t)$ is the force excitation depending on the time parameter t, m is the mass, c the damping coefficient and $\Phi(x, \dot{x})$ is the restoring force expressed by

$$\Phi(x, \dot{x}) = \alpha k x(t) + (1 - \alpha) k z(t) \tag{2}$$

$$\dot{z} = A\dot{x} - \beta \dot{x} |z|^n - \gamma |\dot{x}| z |z|^{n-1} \tag{3}$$

The auxiliary variable z allows one to introduce a smooth hysteretic behavior; k is the pre-yielding stiffness, α represents the ratio between post and pre-yielding stiffness, managing all the intermediate yielding states. In particular, $\alpha = 1$ provides an elastic response and $\alpha = 0$ an elastic-perfectly-plastic behavior. A, β, γ, n are time invariant parameters defining the amplitude and the shape of the cycles, the linearity in unloading and the smoothness of the transition from the pre- to the post-yield region. In detail, A is related to the initial stiffness, β adjusts the cycle amplitude and, as a result, the dissipation level ($\beta \rightarrow 0$ is employed for low energy dissipation), γ defines the unloading path in the hysteresis, n the smoothness of the transition.

The consequential relationship between the model parameters that appear in equation (3) and the resulting shape of the obtained hysteresis loops is detailed in [7] using a special form of the BW model with normalization.

Division by m leads to a more classical form of the second order differential equation (1) in terms of the circular frequency ω_0 and the damping ratio ζ:

$$\ddot{x} + 2\zeta\omega_0\dot{x} = \frac{f(t) - \Phi(x,\dot{x})}{m} \tag{4}$$

Re-arranging the governing equation (4) in the state space form, the following is obtained:

$$\frac{d}{dt}\begin{bmatrix} z \\ u_1 \\ u_2 \end{bmatrix} = \begin{bmatrix} 0 & 0 & A \\ 0 & 0 & 1 \\ -(1-\alpha)\omega_0^2 & -\alpha\omega_0^2 & -2\zeta\omega_0 \end{bmatrix}\begin{bmatrix} z \\ u_1 \\ u_2 \end{bmatrix} + \begin{bmatrix} -\beta u_2|z|^n - \gamma|u_2|z|z|^{n-1} \\ 0 \\ 0 \end{bmatrix} + \begin{bmatrix} 0 \\ 0 \\ m^{-1} \end{bmatrix} f(t) \tag{5}$$

where $u_1 = x$ and $u_2 = \dot{x}$. The state space formulation is usefully employed for numerical implementation in standard computation environments, also going from single to multi-degree-of-freedom systems.

Several developments of the initial formulation of the BW model can be found in literature, among the others, for reproducing stiffness degradation in hysteretic systems [8], to recover Drucker postulate [9]. Next studies result in comprising additional terms and representing the pinching behavior, as observed in reinforced concrete and masonry structures [10, 11]. The biaxial extension was proposed on reinforced concrete beams [12] and 3D frames [13]. More recently the dynamic stability of the model has been investigated in [14], where the domain limits for the model parameters are fixed, the model passivity, among other general properties, is established in [15]. The nonlinear responses and bifurcations of one-dof BW hysteretic oscillators to harmonic excitations have been also investigated in [16].

Parameters Identification for the BW Model

The identification issue can be approached by considering the physical significance of the parameters which define the BW model of hysteresis. Mass m and pre-yielding circular natural frequency ω_0 of the oscillator are related to pre-yielding stiffness k and the BW parameters α and A by the following equation:

$$\omega_0^2 m = k[\alpha + A(1 - \alpha)] \tag{6}$$

Equation (6) is derived from the time derivative of equation (2) where $\dot{z}$ is replaced by its value when $z=0$. Consequently, equation (6) is the ratio between the restoring force $\Phi(x,\dot{x})$ and relative displacement derivative with respect to time, i.e. $\dot{x}$.

The identification of remaining parameters, namely γ and β, can be fixed by setting to zero the derivative $\dot{z}$ (simplifying by $\dot{x}$) and replacing the expression for z as obtained in equation (2). In light of this comment, the following relation results:

$$\Phi_y = \left[\frac{A}{\gamma + \beta}\right]^{\frac{1}{n}} (1 - \alpha)k + \alpha k x \tag{7}$$

From the definition of elastic force and equation (6) one obtains

$$\Phi_y = \left[\frac{A}{\gamma + \beta}\right]^{\frac{1}{n}} (1 - \alpha)k + \alpha k \frac{\Phi_y}{k[\alpha + A(1 - \alpha)]} \tag{8}$$

With A=1 equation (8) can be rewritten as:

$$\Phi_y = \left[\frac{1}{\gamma + \beta}\right]^{\frac{1}{n}} k \tag{9}$$

and equation (6) becomes

$$\omega_0^2 m = k \tag{10}$$

Equation (9) allows to define different yielding levels of the general BW signature, mainly focusing on the hysteresis cycle amplitude definition rather than on the theoretical elastic limit [8].

The parameters can satisfy the physical and mathematical consistency of the general passive BW formulation in equation (3), verifying some properties from [17] such as bounded stability of input and output, passivity among the others. More details can be also found in [6]. Figure 1 depicts different cycles of hysteresis reproduced by the BW model with essential parameters $A = 1$, $n = 1$, $\alpha = 0.0$, $\beta = \gamma = 40$ m^{-1}, $k = 80000$ kN/m, $\Phi_y = 1000$ kN. Influence of their variation has been highlighted in Figure 1.

Lund-Grenoble Friction Model

Friction is a natural phenomenon that is quite complicate to model and it is also an important aspect of many control systems which are able to dissipate mechanical energy by hysteresis cycles, decoupling dynamic motion of the controlled object from its supports, and for high quality servo mechanisms and hydraulic systems as well. Consequently, an accurate model of such behavior results necessary to analyze stability, predict limit cycles and perform simulations among the others.
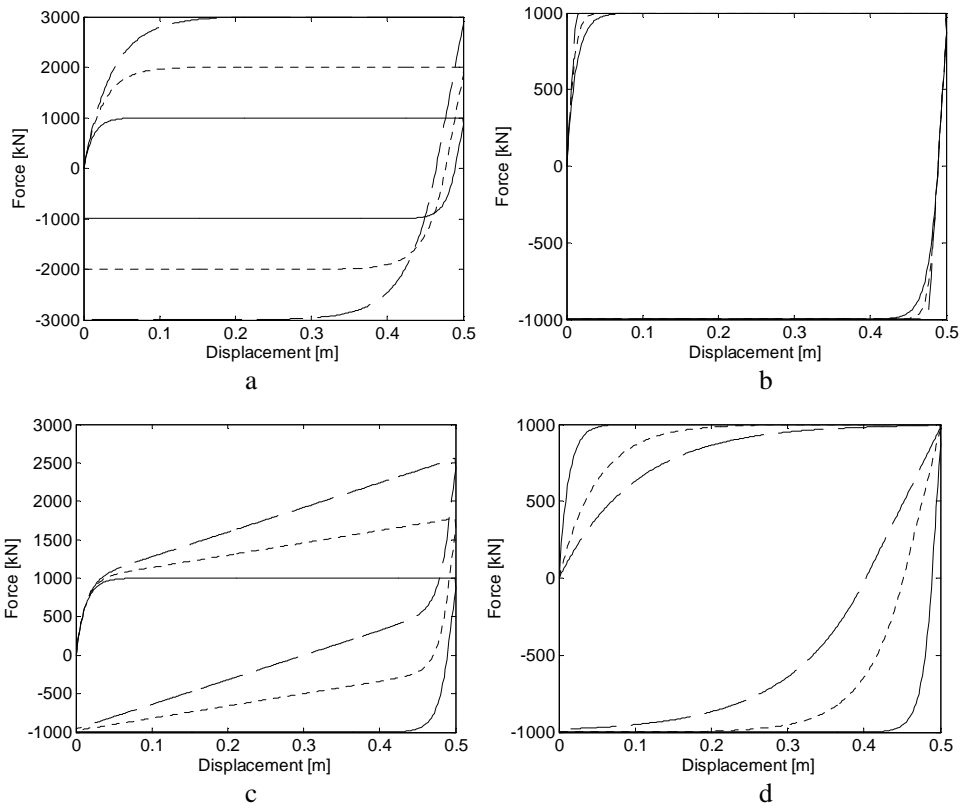
Figure 1. Hysteresis cycles reproduced by BW model: Φ_y = 1000, 2000, 3000 kN (a); n = 1, 2, 10 (b); α = 0.0, 0.02, 0.04 (c); k = 80000, 20000, 10000 kN/m (d).
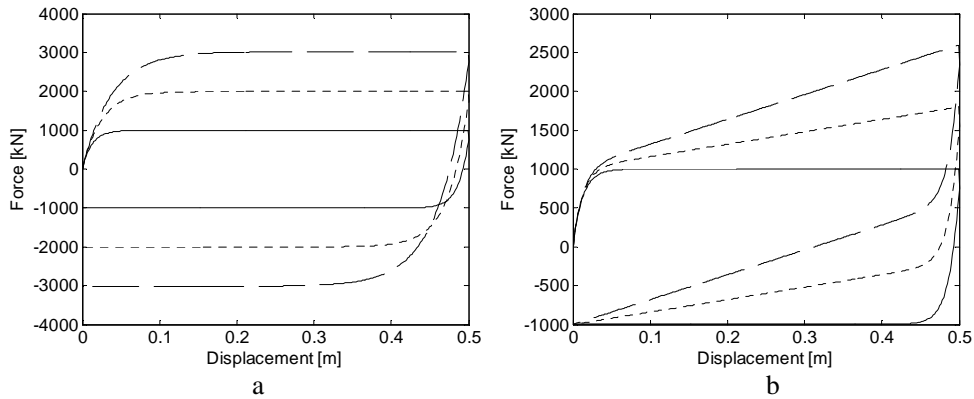

Figure 2. Hysteresis cycles reproduced by LuGre model: (a) with different yielding limits (1000, 2000, 3000 kN respectively through α = 80, 40, 26.5 m^{-1}) and post-yielding behavior k=0, 80000x0.02, 80000x0.04 kN/m.

Classical friction models, such as Coulomb and viscous friction, can be useful in a number of existing numerical schemes. However, in applications with high precision positioning and with low velocity tracking, a more refined model is necessary.

The Lund-Grenoble (LuGre) model [18, 19] allows for a better description of the friction phenomena for low velocities and especially when crossing zero velocity occurs. Efficient simulations of a dynamic systems and control dampers are reported in literature (e.g. [20, 21]). The following relations summarize the LuGre model:

$$\dot{z} = \dot{x} - \alpha \left| \dot{x} \right| z$$

(11)

$$V = \beta z + \zeta \dot{x} + kx + \varepsilon z + V_0$$

(12)

where x is the state variable of the system, z the auxiliary variable, k is the pre-yielding stiffness and ζ the damping coefficient, V is the force and α, β, ε are parameters defining amplitude and shape of the cycles. Figure 2 depicts different cycles of hysteresis reproduced by the LuGre model with basic parameters $\alpha = 80$ m^{-1}, $\beta = 80000$ kN/m, $\zeta = k = \varepsilon = V_0 = 0$.

Modeling Base Isolation Systems

Among control systems, seismic isolation ones are probably the most known and adopted with succesful real world applications. Technology spreads from rubber bearings to pendulum systems, even if some peculiar innovations can also be noted (e.g. [22]). Due to their reliable efficient behavior for protecting civil structures from earthquake loadings, isolation system solutions are also studied for special structures such as nuclear power plant buildings with some interesting applications. Furthermore, a consolidated interest on such control solutions covers different fields from research to recently proposed design standards [23].

In this light, as it is well known, high damping rubber bearings (HDRB) show an interesting non-linear mechanical behavior with hysteresis, characterized also by the scragging and Mullins' effects (stiffness and damping degradation) by the horizontal stiffness variation (due to temperature and axial load), by strain-rate dependence and ageing.

Precursor of a large family of numerical models for isoslation systems simulation, Ozdemir and Wen models [24, 25] of smooth hysteresis are probably the most eclectic phenomenological model presented in the present literature. Thanks to their physical and mathematical consistency, with an excellent correspondence between the experimental and numerical results, a number of developments have been established, from their original formulation, including new features and reproducing new technologies [26, 5].

An excellent overview on the present isolation knowledge, including some issues on modeling and analysis options as well, can be found in the research report by Grant et al. [27]. The main characteristics of a seismic isolation system are described, listing several models for the unidirectional numerical simulation. In conclusion, a bidirectional model is also proposed for representing the bearings response to 2D horizontal loading in terms of stiffness, damping and degradation, on the basis of a decomposition of the bearing resisting force as the sum of an elastic component (from Mooney-Rivlin strain energy function) and an hysteretic force.

A non-differential unidirectional model for elastomeric isolation bearings has been proposed by Kikuchi and Aiken [28] as a development from the Fujita one, in order to improve the performance into the large strain range.

The Fujita model has the characteristic of including a procedure to update model parameters, in contrast with other differential models as Ozdemir or Wen one [24, 25]. The modeling approach proposed by Kikuchi and Aiken modifies the Fujita one in order to improve the performance of the modeling outcomes at high shear strain levels; however the effects of strain rate and of variation of axial load on the bearing hysteresis properties are neglected.

Hwang et al. [29] developed an analytical unidirectional model from the proposed approach by Pan and Yang [30]. In this last, the shear force experienced by the isolator is attributed to the sum of a restoring force, describing the skeleton curve, and a damping force, adopted to represent the area of the hysteresis loop. Such model, however, results unable to reproduce the Mullins and describe the scragging effect on the isolation bearings. The development by Hwang et al. model for high damping elastomeric isolation devices is aimed to overcome such limits. Resoring and damping components of the original Pan and Yang model result modified to describe the stiffness degradation and the decrease of loop area trough a special integral term which accounts the energy dissipated by the elastomeric material or bearing during cyclic loading reversals. Nevertheless, the proposed approach neglects axial loads influence, as well as the rubber compounding and vulcanization process, which can also control the hysteresis behavior of elastomeric isolation bearings. The model parameters identification is also not included in this study, which is mainly focused on the prediction of the force-displacement hysteresis.

The unidirectional model for HDRBs by Tsai et al. [31] has been developed by modifying the Wen model to include rate-dependent effects under constant axial loads. Consequently, it has a differential signature. In spite of the good correlation between experimental and numerical results, the model by Tsai et al. does not show the stiffness and damping degradations, which are distinctive features of such devices.

An unidirectional model for HDRBs under constant axial load is proposed by Jankovsky in [32] accounting nonlinear rate dependent effects. I consists in a non-differential model, developed as well from the Pan and Yang solution [30]. The shear stiffness, K, and damping, C, coefficients at a given time, t, are obtained based on the actual values of displacement, $x(t)$, and velocity, $\dot{x}(t)$ as follws:

$$K(x(t),\dot{x}(t)) = a_1 + a_2 x^2(t) + a_3 x^4(t) + \frac{a_4}{\cosh^2(a_5\dot{x}(t))} + \frac{a_6}{\cosh(a_7\dot{x}(t))\cosh(a_8 x(t))} \tag{13}$$

$$C(x(t),\dot{x}(t)) = \frac{a_9 + a_{10}x^2(t)}{\sqrt{a^2{}_{11} + \dot{x}^2(t)}} \tag{14}$$

where a_1-a_{11} are parameters to be defined for fitting experimental data (e.g. by least squares method). In particular, a_1 is related to the basic stiffness level which is modified by a_2 and a_3 for higher shear strains, a_4 and a_5 control the stiffness at the maximum displacements; a_6-a_8 increase stiffness value in case of motions with lower amplitudes; $a_9 - a_{11}$ manage damping value so as to obtain appropriate hysteresis loops. It has been proved how cyclic experimental tests are well reproduced by the model, even though its performance gets worse when a seismic signal is applied (see Figure 3 with a_1=212390 N/m, a_2=3431000 N/m^3, a_3=-8767000

N/m^5, a_4=518290 N/m, a_5=4.3595 s/m, a_6=586760 N/m, a_7=3.9664 s/m, a_8=91.482 1/m, a_9=15377 N, a_{10}=408680 N/m^2, a_{11}=0.13985 m/s). The adopted parameters have been collected in an example of application from [32] (Example 2).

Abe et al. [33, 34] proposed differential hysteretic models of laminated rubber bearings, HDRB, lead-rubber bearings (LRB) and natural rubber bearings (NRB), under biaxial and triaxial loading conditions on the basis of experimental results.

Firstly, an unidirectional model is derived by extending the Ozdemir [24] elasto-plastic model; secondly, a bidirectional model of the bearing is developed by including symmetric components of the characteristic matrix.

The restoring force for the device unidirectional model is the sum of three contributions: an elastic-plastic model (F_2 hysteretic component) and two elastic non-linear springs, namely a non-linear elastic spring (F_1) and a hardening spring (F_3).

From an analytical point of view the force-displacement relation for the first non-linear spring reads

$$F_1 = K_1 \left\{ \beta + (1-\beta)\exp(-\frac{U_{max}}{\alpha}) \right\} U + a\left[1 - \exp(-b|U|)\right]\mathrm{sgn}(U)$$

(15)

where U is the relative displacement while K_1, a and b are parameters. In Equation (15), the first term reproduces the force linear evolution, while the second one the non-linear behavior.

The hysteretic contribution F_2 is described by the following differential equation

$$\dot{F}_2 = \frac{Y_t}{U_t}\left\{ \dot{U} - |\dot{U}|\left|\frac{F_2}{Y_t}\right|^n \mathrm{sgn}(\frac{F_2}{Y_t}) \right\}$$

(16)

where the Y_t and U_t parameters are in turn defined as

$$Y_t = Y_0(1+\left|\frac{U}{U_H}\right|^p) \quad U_t = U_0(1+\frac{U_{max}}{U_S})$$

(17)

being Y_0 is the initial yielding force, U_0 the initial yielding displacement, U_H the displacement where hardening starts, U_S a parameter for controlling the degradation of the elastic stiffness of the elastic-plastic spring, U_{max} the maximum displacement experienced during the loading history and p a parameter governing the shape of the hardening branch.

Finally a further non-linear spring is introduced in parallel for capturing the increment of the tangential stiffness experienced by the devices at very high strain levels. This results in the F_3 contribution, defined as

$$F_3 = K_2 \left|\frac{U}{U_H}\right|^r U$$

(18)

where r is the parameter to prescribe the shape of the hardening curve, K_2 a constant to describe the contribution of the hardening spring to the total stiffness.
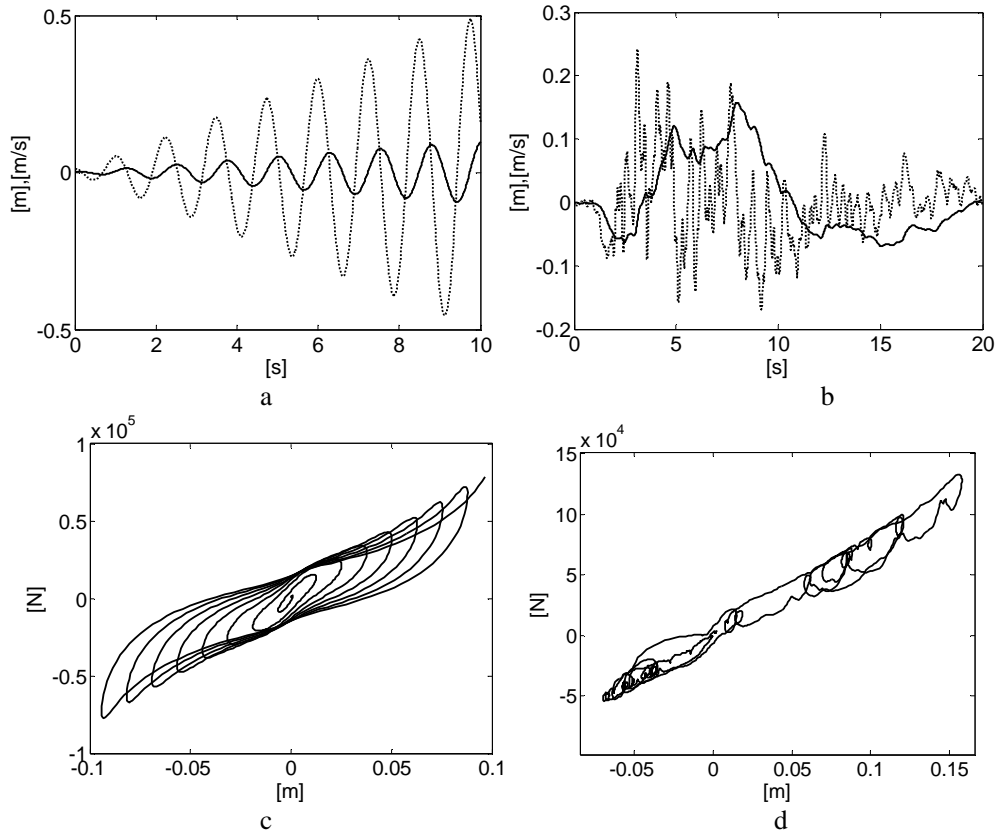
Figure 3. Non-differential unidirectional Jankovsky model: cyclic loading (a) produces the model response (c). Seismic input (b) the model response (d). Dotted lines in (a) and (b) denote velocity.

Details on these model components can be found also in [23] where it has been designated for isolation system simulation under a nuclear power plant building.

Figure 4 depicts the Abe et al. model response (with K_1=1.51 KN/mm, α=8.97 mm, β=0.301, a=9.5 KN, b=0.0675 1/mm, n=0.451, Y_0=13.7 KN, U_h=52.1 mm, p=4.17, U_0=2.07 mm, U_s=30.4 mm, K_2=0.21 KN/mm, r=1.73) under the same cyclic and seismic condition of Figure 3 for comparison. The adopted parameters have been collected in an example of application from [34] (HDR-D sample). Comparing Figures 3 and 4, even if the models reproduce different devices from literature, the seismic response of the non-differential model is questionable. Besides the tests from Figures 3 and 4, several others have been conducted at different amplitudes: it can be concluded that the differential approach results more accurate in the simulation of the device response under seismic-type loading histories; conversely, both unidirectional models [32] and [33, 34] perform similarly when cyclic loading are considered. Ryan et al. in [35] approach the problem of the influence of the axial load variation on the isolator response. In particular the horizontal stiffness and yielding strength have been deepen. They underlined for both HDRB and LRB isolation devices the following considerations: (i) lateral stiffness decreases with the increasing axial load; (ii) lateral yield strength decreases with decreasing axial load (LRB only); (iii) vertical stiffness decreases with increasing lateral deformation.
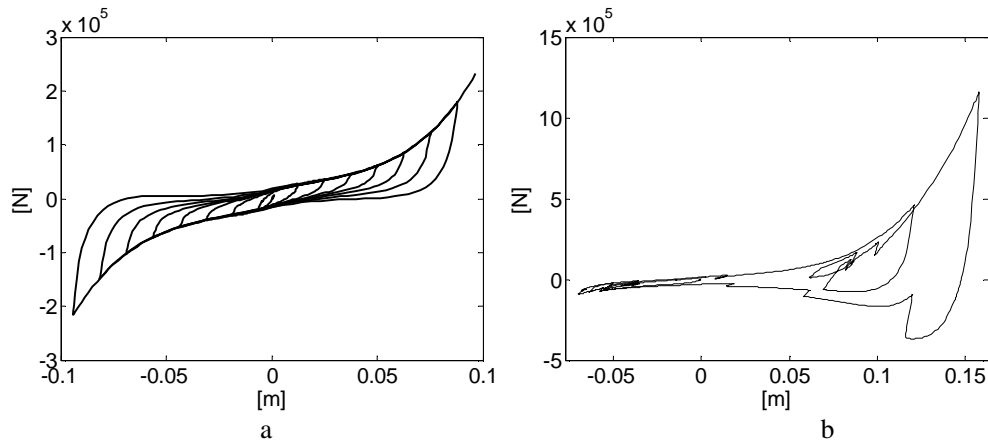
Figure 4. Differential unidirectional Abe et al. model: cyclic loading (Figure 3a) response (a) and seismic (Figure 3b) response (d).

Considerations on HDRB and LRB numerical modeling are also included. Note that the proposed solutions, although an improvement in the isolation knowledge, are declared in [35] as an incomplete representation of the experimental response.

However this literature study can be considered original and of interest for deepening the influence of axial load variation on the isolators response, accounting also different technologies.

Besides the study by Ryan et al., the one by Yamamoto et al. [36] proposes a two-dimensional model for the numerical simulation of seismic isolation bearings including also the influence of axial load. Such model is based on an analytical approach comprising shear and axial springs, having properties which vary with the vertical load.

In particular, the dependence of axial loads is captured by the material nonlinearity formulation of the axial springs and by the transversal geometric nonlinearity of the shear stiffness.

A three dimensional development of this model has been reported in [37]; however, it has to be noted that no evaluation of the model performance is given under three dimensional loading paths (e.g. circular or 8-shaped in the horizontal plane) and/or seismic loads.

Among the approaces herein summarized, the one proposed by Abe et al. [33, 34] seems the most promising for base isolation behavior reproduction in complex structural models. It has been selected in [23] due to its good representation of the experimental response for both cyclic and seismic loading, particularly when bidirectional loading paths in the horizontal plane are considered.

It could also represented an interesting enhancement with respect to simplest bilinear models of isolators, as proposed in existent standards (see [23] for references).

This choice is oriented to eliminate part of uncertainties related to the simulation of the isolation system, being the numerical approach by Abe et al. strictly associated to the actual behavior of the devices.

THE SEMI-ACTIVE MODEL OF HYSTERESIS

The Semi-Active Choice in the Structural Control Discipline

Semi-active approaches for structural control show several good points in comparison with passive and active solutions, which should be underlined as follow [1, 38, 39]:

1   improvement of passive solutions by online adjustments of the damping or stiffness; this is done according to feedback signals and control commands.
2   simplification of the design and the implementation of control systems in comparison with active solutions; this is also due to their requirements of low power supply and low maintenance costs.

Specifically, passive systems have the advantage of being generally more robust than active systems because they are independent from external power sources and processed commands. They perform with fewer operating costs and require a lower maintenance. Their main disadvantage is their inability to adapt to different intensities of excitation. To overcome this limit, semiactive control schemes can be implemented on structural systems.

Semi-active control strategies share the same advantages as passive systems, requiring only a limited amount of active external power to modify the working parameters of the semiactive control devices. This is contrary to the active control case, in which the external power is used to directly inject mechanical energy in the structure through the reactions at the device ends.

Semi-active systems can also be employed in *decentralized* configurations where the whole control system is subdivided into a number of subsystems. When decentralization is employed, e.g. for space structures as long-span bridges, low-order control laws represent a suitable choice. Such algorithms for control force computation are low-order in the sense that they only use the feedback from the nodes that are directly influenced by the devices [38].

Decentralization of control systems, compared to its centralization, presents several good points, of which two in particular have to be underlined:

1   decentralised control systems perform satisfactorily even under adverse conditions showing interesting robust qualities. When local failures occur, if the system is totally decentralized, none of the devices depends on any other. It is therefore acceptable to foresee the failures of one control device at a time, mantaining the global efficency of the control system by the remaining ones.
2   Furthermore, the advantages of designing decentralized control schemes result from the reduction of transmission costs within the feedback loops, the reduction of the overall computational effort and the possibility of a more effective power supply to the devices.

Another intersting classification related to semi-active control systems, but not exclusively, is related to their *collocated* configuration. It occurs when the processed control forces act along the same degree of freedom along which the monitoring data are collected. On the contrary, the system is termed as *non-collocated*.

Toward the Semi-Active Implementation

Smart semi-active device typologies, as those electro-inductive (EI) and electro-magnet-rheological ones (EMR) can be effectively simulated by numerical models [19, 40]. The existent literature develops appropriate rheological models by connecting together simple elements, as spring and dashpot, with non linear parts, depending on the intrinsic characteristics of the device (e.g. viscous, hysteretic or elastic). Some research works report on the force's hysteretic component of real devices which are efficiently reproduced by differential models: among others, the BW one plays a major role, being able to perform with reasonable efficacy [6]. The overviewed solutions adopted for simulating conventional semi-active dampers, as the EI and EMR devices, are able to reproduce the inherent characteristics of the physical systems, consequently improving their knowledge. However, such devices are also able to modulate their dissipation capability, increasing and decreasing online the hysteretic cycles amplitude by external commands, operating simultaneously with the external excitation and adapting themselves to the structural conditions.

Consequently, the development of an operational method for modifying in real time the BW hysteresis cycles, through suitable semiactive laws, may have consequences of practical interest.

In [6] an innovative analytical approach for controlling, by a modified semi-active version of the Bouc-Wen model, the hysteresis component of simulated semi-active control systems is first presented. The next section is devoted to present it.

A General Approach to Semi-Active Modeling

As introduced in previous section, semi-active devices can be regarded as passive ones able to adjust their reaction on-line with the external excitation, through suitable algorithms. Managing their intrinsic dissipation level or stiffness, removing energy from the system or decoupling the structural motion from the base external excitation, they have been shown to significantly outperform the passive schemes by a moderate energy supply. Their practical installation in a wide variety of structures demonstrates their positive function on alleviation of wind and seismic response of buildings, sometimes showing better performances than active systems, which usually are considered the best performers in terms of internal forces and displacements reduction. Acting simultaneously with the hazardous excitation, they also provide enhanced structural behavior for improved usefulness and safety, making the semi-active techniques a very attractive choice for buildings whose functionality is of paramount relevance [6, 38].

The numerical simulation of control devices allows evaluating their efficiency into complicated structural systems, as high-rise buildings or long-span bridges, under a wide variety of external forces. For improving the normal solutions adopted for simulating conventional semi-active dampers, in [6] an operational method for modifying in real time the hysteresis cycles has been first developed, through suitable semi-active laws embedded into the BW numerical model, with promising consequences for buildings.

When semi-active systems are employed in real applications, the information collected from the monitoring system is processed by suitable algorithms. Subsequently, the damper configuration is modified so as to exert the necessary control reactions.

The same procedure can be translated into the simulation environment, where the BW model parameters are updated to modify, as needed, the hysteresis forces which represent the control actions during the real time mock-up. The methodology in [6], for embedding semi-active algorithms and achieving the resulting semi-active BW expression, considers three different control laws, suitable for managing dissipative devices: the *on/off SkyHook*, the *continuous SkyHook*, the *BangBang*. An innovative one, called *continuous BangBang,* is also introduced. The proposed procedure has been demonstrated effective for managing, in real time, the hysteresis component of semi-active systems defining a semi-active version of the BW model, termed for brevity as DM (DoManeschi) model.

The general formulation of the DM model can be summarized by the following equations:

$$F = \alpha k \left(x_{bc} - x_{sup} \right) + (1-\alpha)kz + c \left(\dot{x}_{bc} - \dot{x}_{sup} \right) \tag{19}$$

$$\dot{z} = A \left(\dot{x}_{bc} - \dot{x}_{sup} \right) - \overline{\beta} \left(\dot{x}_{bc} - \dot{x}_{sup} \right) |z|^{n} - \overline{\gamma} \left| \left(\dot{x}_{bc} - \dot{x}_{sup} \right) \right| z |z|^{n-1} \tag{20}$$

$$\overline{\gamma} = f \left(\gamma_{low}, \gamma_{high}, h \right) \tag{21}$$

$$\overline{\beta} = f \left(\beta_{low}, \beta_{high}, h \right) \tag{22}$$

The variable *z* is the auxiliary BW variable allowing to introduce a smooth hysteretic behavior in the control force *F*, x_{bc} and x_{sup} are respectively the coordinate of the body mass to be controlled and the support where the device is connected, *k* the pre-yielding stiffness, *α* the ratio between post and pre-yielding stiffness (*α* =1 provides an elastic response and *α*=0 an elastic-perfectly-plastic behavior), *A* an *n* are time invariant parameters, *c* is the intrinsic viscous component (not considered in the remaining of this chapter).

Parameters $\overline{\gamma}$, $\overline{\beta}$ embeds the general semi-active control law into the BW model for hysteresis modulation defining its semi-active version. They are functions of the BW model parameters *γ*, *β* which control the dissipation level, ranging from the high and low limits (γ_{high} β_{high}, γ_{low} β_{low}) which define the semi-active domain, and the adopted *h* gain [6]. Algorithms can be introduced through equations (21) and (22), guaranteeing mathematical consistency and passivity of the resulting formulation.

Considering the *continuous BangBang* , the following equations replace (21) and (22) ones [6]:

$$\overline{\gamma} = \gamma_{low} + H\left[\left(x_{bc} - x_{sup} \right) \left(\dot{x}_{bc} - \dot{x}_{sup} \right) \right] \left\{ \min \left[\gamma_{low}, \max \left(\left| h\dot{x}_{bc} \right|, \gamma_{high} \right) \right] - \gamma_{low} \right\} \tag{23}$$

$$\overline{\beta} = \beta_{low} + H\left[\left(x_{bc} - x_{sup} \right) \left(\dot{x}_{bc} - \dot{x}_{sup} \right) \right] \left\{ \min \left[\beta_{low}, \max \left(\left| h\dot{x}_{bc} \right|, \beta_{high} \right) \right] - \beta_{low} \right\} \tag{24}$$

The device yielding force level is modulated through $\bar{\gamma}, \bar{\beta}$ parameters in equation (19) and equations (23) and (24); $H[.]$ is the *Heaviside* step function.

The discrete *BangBang* semi-active configuration of the BW model is defined by the following expressions [6]:

$$\bar{\gamma} = \gamma_{low} - \Delta \gamma H\left[\left(x_{bc} - x_{sup}\right)\left(\dot{x}_{bc} - \dot{x}_{sup}\right)\right]$$ (25)

$$\bar{\beta} = \beta_{low} - \Delta \gamma H\left[\left(x_{bc} - x_{sup}\right)\left(\dot{x}_{bc} - \dot{x}_{sup}\right)\right]$$ (26)

Two values can be assumed by $\bar{\gamma}, \bar{\beta}$ parameters, depending whether the high or the low state for damping is required and the increments are defined as $\Delta\gamma = \gamma_{low} - \gamma_{high}$ and $\Delta\beta = \beta_{low} - \beta_{high}$.

In analogy with the last one, the discrete semi-active on/off *SkyHook* configuration of the BW model results [6]:

$$\bar{\gamma} = \gamma_{low} - \Delta \gamma H\left[\dot{x}_{bc}\left(\dot{x}_{bc} - \dot{x}_{sup}\right)\right]$$ (27)

$$\bar{\beta} = \beta_{low} - \Delta \beta H\left[\dot{x}_{bc}\left(\dot{x}_{bc} - \dot{x}_{sup}\right)\right]$$ (28)

Accordingly to [6], the semi-active *continuous SkyHook* form of the BW model is:

$$\bar{\gamma} = \gamma_{low} + H\left[\dot{x}_{bc}\left(\dot{x}_{bc} - \dot{x}_{sup}\right)\right]\left\{\min\left[\gamma_{low}, \max\left(|h\dot{x}_{bc}|, \gamma_{high}\right)\right] - \gamma_{low}\right\}$$ (29)

$$\bar{\beta} = \beta_{low} + H\left[\dot{x}_{bc}\left(\dot{x}_{bc} - \dot{x}_{sup}\right)\right]\left\{\min\left[\beta_{low}, \max\left(|h\dot{x}_{bc}|, \beta_{high}\right)\right] - \beta_{low}\right\}$$ (30)

where $\bar{\gamma}, \bar{\beta}$ parameters can assume continuously variable values between the two high and low limits.

The *h* gain adopted for the continuous semi-active versions (equations (23)-(24) and (29)-(30)) consists in $\gamma_{low} / max(\dot{x}_{body})$, where the denominator is the expected maximum body mass velocity [6].

When semi-active hysteretic control systems are adopted, their ability in energy dissipation and their aptitude in decoupling the support vibration from the body mass are valuable mitigation resources that should be estimated. These properties are also investigated in [6] for the proposed DM model with different configurations. Such observations may improve the semi-active structural control design perspective.

Figure 5 depicts the mean control force and equivalent damping factor for semi-active dampers with identical sinusoidal input time histories, at increasing amplitudes, for reproducing a standard motion of the dampers connection points.
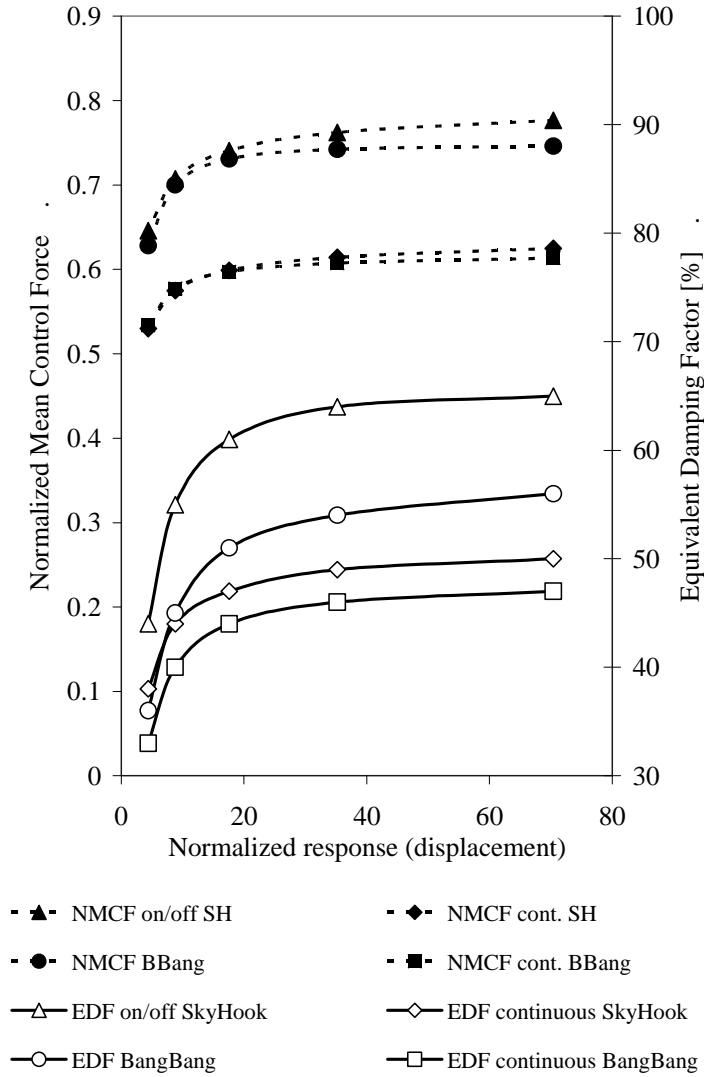
Figure 5. Restrain and dissipation vs. different input cycle amplitudes.

Forces and displacements are here normalized to the device highest yielding level. Four different control algorithms are implemented: the *SkyHook*, the continuous *SkyHook*, the *BangBang* and the continuous *BangBang* law through the following parametes: $A=1$, $n=1$, $\alpha=0$, the yielding forces $\Phi_y=1000kN$ and $500kN$ respectively for the high and low semi-active limit, $k=80000kN/m$, with $\gamma_{low}=\beta_{low}$ and $\gamma_{high}=\beta_{high.}$. A significant decoupling of relative motions between the support and body mass to be controlled, with respect to the discrete algorithms, is exerted by the continuous semi-active laws; on the contrary, highest dissipation levels are provided from the discrete ones.

The BW model in its original formulation, from which the DM one has been derived, has proven to perform with reasonable efficiency in reproducing the force's hysteretic component

of real passive device, playing a major role among other differential ones. It can reproduce also the hysteresis signature coming from a wide range of semi-active damper technologies, e.g. an innovative EI one characterized in laboratory for structural control applications on bridges [19]. It represents a fascinating solution for the feasibility of larger passive devices of this type to be installed in long span bridges. This is of interest due to two facts: that they are much shorter than passive hydraulic dampers of identical maximum stroke and that they can easily be converted into the semi-active type, adapting themselves to different seismic intensity levels by using specific control laws. An additional aspect to be underlined of such devices is the self-centering ability after an extreme loading event, realigning the deck with its original axis and the towers.

Figure 6 depicts some input kinematic conditions with standard sinusoidal shapes for the proposed semi-active models of hysteresis. Namely the continuous line is the sinusoidal motion in terms of displacements for the support and the body mass to be controlled (x_{bc} and x_{sup} respectively). Figure 7 reports the hysteresis response of the models. The BW parameters have been set as those in Figure 5 ($A=1$, $n=1$, $\alpha=0$, $\Phi_y=1000$kN and 500kN respectively for the high and low semi-active limit, $k=80000$kN/m, with $\gamma_{low}=\beta_{low}$ and $\gamma_{high}=\beta_{high.}$).

Several results from literature are intended as a realistic validation of such innovative semi-active technology implementation on complex structures by numerical simulations through finite element models. The next section is devoted to summarize some research works where bridge structures in particular are considered.

However, the numerical simulation by suitable models of hysteresis and the detailed approaches are intended to a wide application at different building typologies.

APPLICATIONS EXAMPLES

The previously discussed numerical approaches have demonstrated to be capable to reproduce control systems with passive and semi-active signature in complex structural models (e.g. finite element ones).
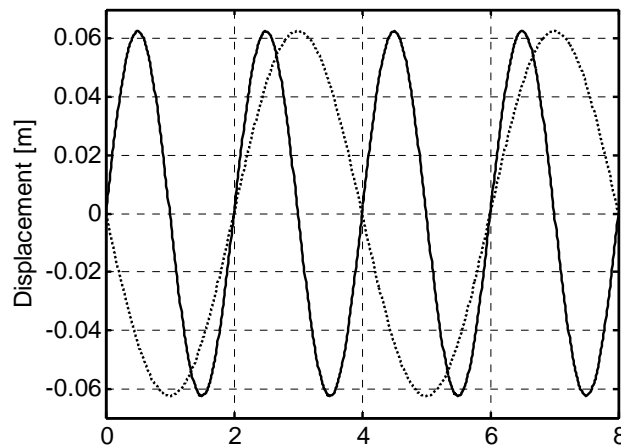

Figure 6. Restrain and dissipation vs. different input cycle amplitudes. Continuous line for the support, dotted for the body mass to be controlled.
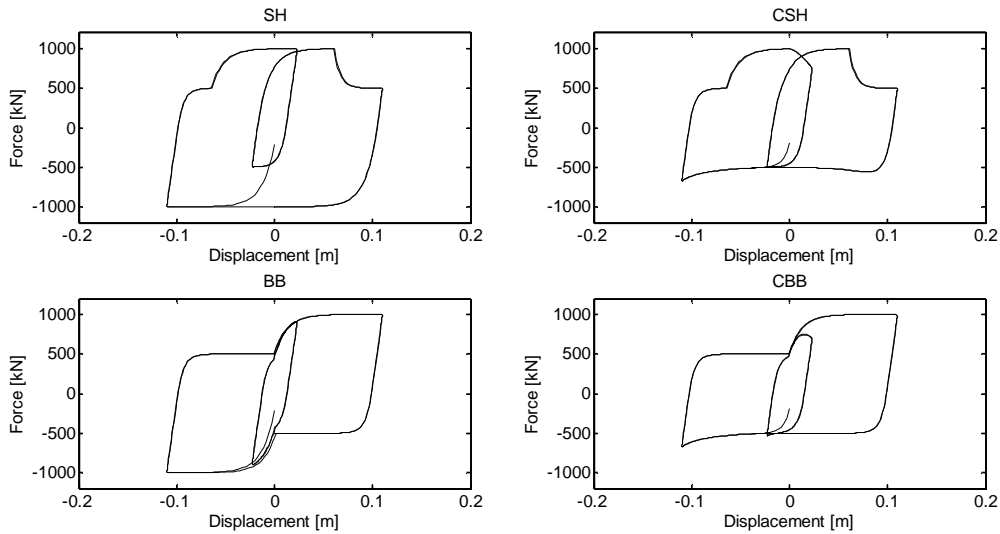
Figure 7. Models response to the sinusoidal input of Figure 6. SH and BB refer to discrete *SkyHook* and *BangBang* models, CSH and CBB respectively to the continuous ones.

Mitigation of direct dynamic effects is traditionally the primary target of control systems (e.g. acceleration and/or displacements mitigation). However, attention is also given to the positive outcomes related to indirect effects coming from the dampers implementation on buildings.

The international control benchmark on cable stayed bridges, attracting in the last years the attention of the control community, has been considered in [38] for studying passive and semi-active decentralized collocated solutions for seismic mitigation. The passive BW and semi-active on/off DM models are employed. Robust feasible solutions are investigated starting from a first step where passive devices are applied to the bridge numerical model between the deck and the piers. Subsequently, an open-loop semi-active improvement of the passive control system is implemented and, finally, an innovative decentralized solution for a semi-active scheme in closed-loop configuration is introduced. The device force displacement relationship fits the results of laboratory tests during the characterization process of an EI device [19].

In [22] the results of simulation tests to identify the mechanical signature of an innovative isolation device known as the Roll-N-Cage (RNC) isolator are presented. The seismic performance of an RNC passive control scheme is subsequently investigated on an updated model of the cable-stayed bridge benchmark. The force–displacement relationship of the device is reproduced using the standard Bouc–Wen model of smooth hysteresis. Subseqently, the numerical assessment of the device efficiency is established through its implementation into a bridge model considering several ground motions as external excitations. It was found that the RNC isolator is promising as a reliable isotropic horizontal isolation device for bridge structures.

The same updated version of the controlled cable-stayed bridges is considered in [41] including new aspects in the knowledge of the relative transversal motion of the main girder with respect to the towers under seismic motions. Earthquake restrainers in the transverse direction are considered in the original benchmark configuration.

The proposed updated bridge model first reproduces this kinematic arrangement, subsequently this restriction has been overcome and a new configuration with transversal releases is studied. The control strategies consist in passive and decentralized semi-active systems working in the horizontal plane, likewise those studied for the original statement in the previous investigation [38]. The proposed arrangement schemes markedly mitigate the transversal structural response of the bridge with sensible effectiveness.

The main goal of the study in [42, 43] consists in the evaluation of the control system performance, for iconic bridges, when local failure occurs in the control system devices. Model of a cable-stayed bridge and a suspension one are developed at the numerical level in a commercial finite element code, starting from original data. The models are used to simulate the structural response under extreme loading conditions, such as seismic excitation and wind. Different types of control systems for the mitigation of the bridge response, implementing passive and semi-active dampers respectively, are employed through the BW and MD approaches from the literature.

Some general observations, by means of a proposal for quantitative robustness indexes in terms of control performance, are also provided. Resilience advantages in bridge structures by means of smart control strategies is an innovative research topic currently under investigtion at the Politecnico di Milano.

Collocated and non collocated decentralized control strategies for an existent suspension bridge are studied in [44] against strong wind buffeting adopting a numerical approach. An original procedure for implementing BW and DM models into a multipurpouse finite element code is included by a mixed implicit-explicit step by step formulation. The bridge model results useful to assess the efficacy of passive and discrete semi-active control schemes. Their efficacy in mitigating instant loading effects is shown and the factors contributing to their positive performance both for mitigating instant structural variables and also fatigue damages are highlighted. Protection of composite decks in long span bridges against fatigue damage through decentralized control schemes is an interesting research topic currently under investigation at the Politecnico di Milano.

The numerical model of an existing suspension bridge is used in [45] to reevaluate an optimization procedure for a passive control strategy, already proven effective in [44] with a simplified model of the buffeting wind forces. The BW is used for reproducing the dissipative behavior of the passive control scheme. Such optimization procedure, previously imple-mented with a quasi-steady model of the buffeting excitation, is reevaluated adopting a more refined version of the wind-structure interaction forces. It is based on the use of indicial function, adopting to reflect coupling with the bridge orientation and motion. The final outcomes show that the previously identified optimal passive configuration withstands.

The research work [23] is focused on the development of a numerical procedure for the computation of seismic fragilities in base isolated Nuclear Power Plants. A special procedure for fragility computation is proposed making use of the Response Surface Methodology to model the influence of the random variables on the dynamic response and the Monte Carlo method is used to compute the failure probability. The nuclear building is equipped with a base isolation system based on the introduction of High Damping Rubber Bearing elements showing a markedly non linear mechanical behavior and simulated by the Abe et al. [33, 34]. The isolation devices result the critical elements in terms of seismic risk and the dynamic behavior of the building, belonging to rigid body motion one, is captured by low-dimensional numerical models.

REFERENCES

[1]   Domaneschi, M. (2006). Structural Control of Cable-stayed and Suspended Bridges. *Ph.D. Thesis*. University of Pavia, I. file:///C:/Users/ghisi/Downloads/Domaneschi.pdf.

[2]   Bouc, R. (1967). Forced vibrations of mechanical systems with hysteresis. *Proceedings of the 4th International Conference on Nonlinear Oscillations*. Prague, Czechoslovakia.

[3]   Wen, Y. K. (1976). Method for random vibration of hysteretic systems. *Journal of the engineering mechanics division ASCE*. 102, 249–263.

[4]   Erlicher, S., Point, N. (2004). Thermodynamic admissibility of Bouc–Wen type hysteresis models. *C. R. Mecanique*. 332, 51–57.

[5]   Casciati, F., Faravelli, L. (1991). Fragility Analysis of Complex Structural Systems. *Research studies press ltd*. Taunton, Somerset, England.

[6]   Domaneschi, M. (2012). Simulation of Controlled Hysteresis by the Semi-active Bouc-Wen Model. *Computers and Structures*. 106–107, 245–257.

[7]   Ikhouane, F., Hurtado, J. E., Rodellar, J. (2007). Variation of the hysteresis loop with the Bouc–Wen model parameters. *Nonlinear Dynam*. 48, 361–380.

[8]   Baber, T. T., Wen, Y. K. (1981). Random vibration of hysteretic, degrading systems. *Journal of the engineering mechanics division ASCE*. 107, 1069-1087.

[9]   Casciati, F. (1989). Stochastic Dynamics of Hysteretic Media. *Structural Safety*. 6, 259-269.

[10] Noori, M., Dimentberg, M., Hou, Z., Christodoulidou, R., Alexandrou, A. (1995). First-passage study and stationary response analysis of a BWB hysteresis model using quasi-conservative stochastic averaging method. *Probabilist. Eng. Mech*. 10, 161-170.

[11] Foliente, C. G., Singh, M. P., Noori, M. N. (1996). Equivalent linearization of generally pinching hysteretic, degrading systems. *Earth. Eng. Struct. D*. 25, 611-629.

[12] Park, J., Wen, Y. K., Ang, A. H. S. (1986). Random vibration of hysteretic systems under bi-directional ground motions. *Earthq. Eng. Struct. D*. 14, 543-557.

[13] Casciati, F., Faravelli, L. (1998). Stochastic equivalent linearization for 3D frames. *J. Eng. Mech. ASCE*. 114, 1760-1771.

[14] Ikhouane, F., Manosa, V., Rodellar, J. (2007). Dynamic properties of the hysteretic Bouc-Wen model. *Syst. Control. Lett*. 56, 197–205.

[15] Ismail, M., Ikhouane, F., Rodellar, J. (2009). The hysteresis bouc-wen model, a survey. *Arch. Comput. Method. E*. 16, 161–188.

[16] Lacarbonara, W., Vestroni, F. (2003). Nonclassical Responses of Oscillators with Hysteresis. *Nonlinear Dynam*. 32, 235–258.

[17] Ismail, M., Ikhouane, F., Rodellar, J. (2009). The hysteresis Bouc-Wen model, a survey. *Arch. Comput. Method. E*. 16, 161–88.

[18] Canudas de Wit, C., Olsson, H., Astrom, K. J., Lischinsky, P. (1995). A New Model for Control of Systems with Friction. *IEEE Transactions on Automatic control*. 40(3), 419-425.

[19] Casciati, F., Domaneschi, M. (2007). Semi-active Electro-inductive Devices: Characterization and Modelling. *Journal of Vibration and Control*. 13(6), 815-838.

[20] Boston, C., Weber, F., Guzzella L. (2010). Modeling of a disc-type magnetorheological damper. *Smart Mater. Struct*. 19, 045005, 12pp.

[21] Do, N., Ferri, A., Buachau, O. A. (2007). Efficient Simulation of a Dynamic System with LuGre Friction. *Journal of Computational and Nonlinear Dynamics.* 2, 281-289.

[22] Ismail, M., Rodellar, J., Carusone, G., Domaneschi, M., Martinelli L. (2013). Characterization, modeling and assessment of Roll-N-Cage isolator using the cable-stayed bridge benchmark. *Acta Mechanica.* 224, 525–547.

[23] Perotti, F., Domaneschi, M., De Grandis, S. (2013). The numerical computation of seismic fragility of base-isolated NPP buildings. *Nuclear Engineering and Design.* 262, 189–200.

[24] Ozdemir, H., 1976. Nonlinear transient dynamic analysis of yielding structures. *Ph.D. Dissertation,* Division of Structural Engineering and Structural Mechanics, Department of Civil Engineering, University of California, Berkeley.

[25] Wen, Y. K., 1976. Method for random vibration of hysteretic systems. *J. eng. mech. ASCE.* 102. 249-263.

[26] Sivaselvan, M. V., Reinhorn, A. M., 2000. Hysteretic models for deteriorating inelastic structures. *J. eng. mech. ASCE.* 126(6), 633-640.

[27] Grant, D. N., Fenves, G. L., Auricchio, F. (2005). Modelling and analysys of high-damping rubber bearings for the seismic protection of bridges. *Research Report No. ROSE-2005/01*, ROSE School, Pavia, I.

[28] Kikuchi, M., Aiken, I. D. (1997). An analytical hysteresis model for elastomeric seismic isolation bearings. *Earthquake Engng. Struct. Dyn*. 26, 215-231.

[29] Hwang, J. S., Wu, J. D., Pan, T. C., Yang, G., 2002. A Mathematical Hysteretic Model for Elastomeric Isolation Bearings. *Earthquake Engng. Struct. Dyn.* 31, 771-789.

[30] Pan, T. C., Yang, G., 1996. Nonlinear analysis of base-isolated MDOF structures. *Proceedings of the 11th World Conference on Earthquake Engineering*, Mexico. Paper No. 1534.

[31] Tsai, C. S., Chiang, T. C., Chen, B. J., Lin, S. B., 2003. An advanced analytical model for high damping rubber bearings. *Earthquake Engng. Struct. Dyn.* 32, 1373-1387.

[32] Jankowski, R., 2003. Nonlinear Rate Dependent Model of High Damping Rubber Bearing. *B Earthq. Eng.* 1, 397-403.

[33] Abe, M., Yoshida, J., Fujino, Y., 2004a. Multiaxial Behaviors of Laminated Rubber Bearings and Their Modeling. I: Experimental Study. *J. Struct. Eng.-ASCE.* 130, 1119-1132.

[34] Abe, M., Yoshida, J., Fujino, Y., 2004b. Multiaxial Behaviors of Laminated Rubber Bearings and Their Modeling. II: Modeling. *J. Struct. Eng.-ASCE.* 130, 1133-1144.

[35] Ryan, K. L., Kelly, J. M., Chopra, A., 2005. Nonlinear Model for Lead-Rubber Bearings Including Axial-Load Effects. *J. Struct. Eng.-ASCE.* 131, 1270-1278.

[36] Yamamoto, S., Kikuchi, M., Ueda, M., Aiken, I. D., 2009. A mechanical model for elastomeric seismic isolation bearings including the influence of axial load. *Earthquake Engng. Struct. Dyn*. 38, 157-180.

[37] Kikuchi, M., Nakamura, T., Aiken, I. D., 2010. Three-dimensional analysis for square seismic isolation bearings under large shear deformations and high axial loads. *Earthquake Engng. Struct. Dyn.* 39, 1513-1531.

[38] Domaneschi, M. (2010). Feasible control solutions of the ASCE benchmark cable-stayed bridge. *Structural Control and Health Monitoring.* 17, 675-693.

[39] Casciati, F., Magonette, G., Marazzi, F. (2006). *Technology of semi-active devices and applications in vibration mitigation.* John Wiley and Sons Ltd.

[40] Yang, G., Spencer Jr, B. F., Jung, H. J., Carlson, J. D. (2004). Dynamic modeling of large-scale magnetorheological damper systems for civil engineering applications. *J. Eng. Mech.-ASCE*. 130, 1107–14.

[41] Domaneschi, M., Martinelli, L. (2013). Deepening the ASCE bridge benchmark: transversal response under seismic loading. Accepted in *Journal of Bridge Engineering ASCE*. DOI: 10.1061/(ASCE) 13 BE.1943-5592.0000532.

[42] Domaneschi, M., Martinelli, L. (2014). Robustness of passive and semi-active control schemes on a cable stayed bridge under extreme loading conditions. *7th International Conference on Bridge Maintenance, Safety and Management (IABMAS 2014)*. Shanghai, China, July 7-11.

[43] Domaneschi, M., Martinelli, L., E. Po (2014). Robustness issues and hybridization of a Tuned Mass Damper system on a suspension bridge model under variable wind buffeting. *7th International Conference on Bridge Maintenance, Safety and Management (IABMAS 2014)*. Shanghai, China, July 7-11.

[44] Domaneschi, M., Martinelli, L. (2013). Optimal Passive and Semi-active Control of a Wind Excited Suspension Bridge. *Structure and Infrastructure Engineering*. 9(3):242-259.

[45] Domaneschi, M., Martinelli, L. (2014). Refined Optimal Passive Control of Buffeting-induced Wind Loading of a Suspension Bridge. *Wind and Structures*. 18, 1-20.